CCL299, a benzimidazole derivative, induces G1 phase arrest and apoptosis in HepG2 and HEp-2 cells

（ベンゾイミダゾール誘導体 CCL299 が HepG2 細胞および HEp-2 細胞に誘導する G1 期細胞周期停止とアポトーシス）

千葉大学大学院医学薬学府

先端医学薬学専攻

（主任：白澤浩教授）

大野　吉史

Abstract

Background/Aim: Benzimidazoles are considered as potential anticancer candidates. We studied the anticancer activity of CCL299, 4-(1H-1,3-benzodiazol-1-yl) benzonitrile.

Materials and Methods: In this *in vitro* study, we used ATP assays, flow cytometry, western blotting, and caspase-3/7 assays to evaluate the effects of CCL299 on cell proliferation, cell-cycle progression, and apoptosis.

Results: ATP assays showed that CCL299 inhibited cell growth in the hepatoblastoma cell line HepG2 and the cervical cancer cell line HEp-2, without exhibiting cytotoxic effects on non-cancer cells and TIG-1-20 fibroblasts. Flow cytometry, Western blotting, and caspase-3/7 assays revealed that CCL299 induced G1-phase cell-cycle arrest followed by apoptosis that was associated with the upregulation of p-p53 (Ser15) and p21 expression and the downregulation of p-CDK2 (Thr160) expression.

Conclusion: The results demonstrate that CCL299 exhibits cytotoxic activity via apoptosis in a subset of cancer cells, and should be considered as a promising anticancer candidate agent.

Introduction

Cancer remains a significant cause of death worldwide (1, 2). Understanding the molecular mechanisms underlying cancers has enabled cancer diagnosis and improved patient survival. However, mortality in advanced cancer is partly attributable to tumour insensitivity towards anticancer drugs and due to acquired drug resistance (3-5). Identifying novel compounds with more significant cytotoxicity for cancer cells and fewer side effects is of great importance.

Benzimidazoles are well-known heterocyclic organic compounds containing benzene and imidazole groups. Benzimidazole derivatives are known for their antimicrobial and anti-parasitic activities, and they are potential candidates for anticancer therapy because they can alter tubulin-binding capacity (6-10). Mebendazole contains a benzimidazole skeleton and has been used worldwide as a vermifuge for echinococcosis and giardiasis in humans (11, 12). Mebendazole's potential as an anticancer agent was investigated and it was found to induce inhibition of cancer cell growth via M phase arrest (13-15). Similarly, albendazole, which is used to treat trichuriasis and hookworm infection (16), has anticancer activity that is mediated through M phase arrest in several human cancer cell lines (17-20).

Generally, mammalian cell cycle progression is regulated by cyclin-dependent kinases (CDKs), along with cyclins and CDK inhibitory proteins. CDK2 binds to cyclin

E, and the resultant cyclin E–CDK2 complex promotes G1 phase progression (21). CDK2 activity is strongly controlled by the phosphorylated status of CDK2 at threonine (Thr) 160 (22). p53 and p21 are well known as key CDK inhibitors that are involved in several signalling pathways. Their protein expression levels increase in response to stress signalling and this induces cell-cycle arrest at the G1 phase, followed by apoptosis (23). Therefore, both CDKs and CDK inhibitory proteins are highly validated as anticancer drug targets (24-26).

Chiba Chemical Library is a molecule library that contains more than a thousand compounds, and we have selected several hit compounds as anticancer agents from the library (27-29); among these, 4-(1H-1,3-benzodiazol-1-yl) benzonitrile (CCL299) is one of the benzimidazole derivatives. The anticancer activity of CCL299 in human cancer cells has not been reported until now. The aim of this study was to assess the anticancer effects of CCL299. To accomplish this aim, we compared the cytotoxic effect of CCL299 on both human cancer and non-cancer cells, and investigated the detailed mechanism underlying its anticancer activity, while primarily focusing on the expression of CDKs, p53, and p21.

Materials and Methods

Materials

Chiba Chemical Library provided CCL299 (4-(1H-1,3-benzodiazol-1-yl)benzonitrile; Figure 1A) and CCL937 (1-phenyl-1H-benzoimidazole; Figure 1B) of >95% purity. The compounds were dissolved in dimethyl sulfoxide (DMSO; Fujifilm Wako Pure Chemical Industries, Osaka, Japan) to obtain a 20 mmol/L stock solution. Sodium thiosulfate was purchased from Fujifilm Wako Pure Chemical Industries (Osaka, Japan) and dissolved in phosphate-buffered saline (PBS) to obtain a concentration of 25 mmol/L. For all experiments, the final concentrations were prepared by diluting the stock solutions of CCL299 and CCL937 with DMSO. Control cultures received the same volume of DMSO (0.02%, v/v). Dulbecco's modified Eagle's medium (DMEM) and fetal bovine serum (FBS) were obtained from Thermo Fisher Scientific (Waltham, MA, USA). Primary antibodies against cyclin D1, cyclin E1, CDK2, CDK4, CDK6, Phospho-CDK2 (Thr160), p21, p53, Phospho-p53 (Ser15), and β-actin were purchased from Cell Signaling Technology (Danvers, MA, USA), and secondary antibodies (goat anti-rabbit and horse anti-mouse) were purchased from Jackson ImmunoResearch (West Grove, PA, USA).

Cell lines and cell culture

The human hepatoblastoma cell line HepG2, the human lung adenocarcinoma cell line A549, and human fibroblasts TIG-1-20 were purchased from the National Institutes of

Biomedical Innovation, Health, and Nutrition (Sen-nan, Osaka, Japan). The human cervical cancer cell line HEp-2 (HeLa derivative) was obtained from the Riken Cell Bank (Tsukuba, Ibaraki, Japan). Cells were cultured in DMEM with 10% FBS at 37°C and 5% CO_2 in a humidified atmosphere.

Cell viability assays

Cells were seeded at 2 × 10^4 cells per well in 24-well plates in DMEM with 10% FBS. After 24-h incubation, cells were treated with various concentrations of both the compounds for the indicated periods. ATP assays, using Cell Titer-Glo® Luminescent Cell Viability Assay kit (Promega, Madison, WI, USA), were used to assess cell viability according to the manufacturer's instructions, and the results were read with a microplate reader (Wallac 1420 ARVOsx Multilabel Counter; PerkinElmer, Chiba, Japan).

Flow cytometry analyses of cell cycle

Cells were cultured in a 6-cm dish (3 × 10^5 cells per dish) for 24 h, and then treated with 10 μmol/L CCL299 or DMSO for another 24 hours. Next, cells were collected and washed twice with PBS, treated with reagents from the CycleTEST™ PLUS DNA Reagent Kit (Becton Dickinson and Company, Franklin Lakes, NJ, USA), and analysed

on a BD Accuri™ C6 Flow Cytometer (Becton Dickinson and Company, Franklin Lakes, NJ, USA) that was equipped with a FACScan fluorescence 2 (FL2) detector. The collected data were analysed using FlowJo 7.6.5 (TreeStar Company, San Carlos, CA, USA).

Western blot analyses

Cells were seeded in a 6-cm dish (3×10^5 cells per dish) for 24 h and subsequently treated with 10 μmol/L CCL299 or DMSO for another 24 hours. Then, cells were collected and washed twice with PBS. An equal number of treated and untreated cells were resuspended in an equal volume of M-PER@ Mammalian Protein Extraction Reagent (Thermo Fisher Scientific, Waltham, MA, USA) with a mixture of protease inhibitors (Sigma-Aldrich, Steinheim, Germany) and mixed gently for 10 min. Lysates were centrifuged at 14,000 × *g* for 15 min. Equal volumes of extracted protein were loaded onto SDS-polyacrylamide gels (Atto Corporation, Tokyo, Japan) and transferred onto polyvinylidene difluoride (PVDF) membranes (Trans-Blot Turbo™ Transfer Pack; Bio-Rad, Hercules, CA, USA). After transfer, the PVDF membranes were washed three times with PBS containing 0.1% Tween 20 and incubated with the abovementioned primary antibodies overnight at 4°C. The PVDF membranes were washed again and incubated with a 1:2000 dilution of secondary antibodies for 2 h at

room temperature. Proteins were detected using the ECL plus kit (Bio-Rad, Hercules, CA, USA), and protein bands were detected with ECL Western Blotting Detection Reagents (GE Healthcare, Tokyo, Japan). With β-actin as the control, the relative band intensity was assessed by ImageJ software.

Caspase-3/7 assays

Cells were seeded at a density of 2×10^4 cells per well in 24-well plates in DMEM with 10% FBS. After a 24-h incubation, cells were treated with 10 μmol/L of CCL299 or DMSO for 24 or 36 h. Caspase-3/7 assays using Caspase-Glo® 3/7 Assay kit (Promega, Madison, WI, USA) were used to assess cell caspase activities and read with a microplate reader (Wallac 1420 ARVOsx Multilabel Counter; PerkinElmer, Chiba, Japan) according to the manufacturer's instructions.

Statistical analysis

Statistical analyses were performed using Statcel4, Version 4 (OMS, Tokyo, Japan). All values were expressed as the mean ± standard error (SE) of the results from three biologically independent determinations. Multiple mean values were compared using a single factor analysis of variance (ANOVA) with Dunnett's test or by the two-factor factorial ANOVA. Differences between values were evaluated using the Student's *t*-

test. $P < 0.05$ was considered statistically significant.

Results

Effects of CCL299 on cell viabilities

To compare the cytotoxicity of CCL299 against cancer cells and non-cancer cells, the effects of CCL299 on cell viability were investigated by ATP assays, using HepG2, HEp-2, and A549 cells as the cancer cell lines and TIG-1-20 as the non-cancer cell line. As shown in Table 1, the estimated IC_{50} values after 24-h treatment with CCL299 were 1.0 and 2.7 μmol/L for HepG2 and HEp-2 cells, respectively, and the values for A549 and TIG-1-20 were both >20 μmol/L. In addition, as shown in Figure 2A and 2B, CCL299-mediated suppression of cell growth was dose- and time-dependent in both HepG2 and HEp-2 cells. These results suggested that the growth inhibition by CCL299 might be exhibited only in a subset of cancer cells.

Comparison of CCL299 with CCL937

Compared with the other cancer and non-cancer cells that were tested, HepG2 and HEp-2 cancer cells were more sensitive to CCL299 and, therefore, were used in subsequent experiments. To test whether the cyano group of CCL299 is crucial for the anticancer potential of CCL299, we compared the anticancer ability of CCL299 with

that of CCL937, which shares the core skeleton of CCL299 but has no cyano group. CCL299 induced significant growth inhibition of both HepG2 and HEp-2 cells at 10 μmol/L, whereas CCL937 did not cause growth inhibition under the same conditions (Figure 3A).

The differential cytotoxicities induced by CCL299 and CCL937 suggested that the cytotoxicity of CCL299 might be due to the release of cyanide anions. To test whether cyanide anions were released, we examined the cytotoxicity of CCL299 with or without thiocyanate generation. Sodium thiosulfate attenuates the cytotoxicity of cyanide anions by converting cyanide anions to thiocyanates (30). Cell viabilities were not restored even when sodium thiosulfate (1.0 mmol/L) was added to HepG2 or HEp-2 cells (Figure 3B), indicating that CCL299 would not release cyanide anions under these conditions.

Effects of CCL113 on cell-cycle progression

To evaluate the effect of CCL299 on cell-cycle progression, we next performed fluorescence-activated cell sorting analyses of propidium iodide (PI)-stained cancer cells. As shown in Figure 4A and 4B, compared to vehicle treatment, CCL299 treatment significantly increased the number of cells in the G1 phase (69.9% vs. 59.5% in HepG2 cells and 75.9% vs. 66.1% in HEp-2 cells) and decreased the number of

cells in the S phase (8.1% vs. 21.5% in HepG2 cells and 7.0% vs. 18.2% in HEp-2 cells). However, there was no significant difference in the percentage of cells in the G2/M phase between CCL299-treated cells and control cells. These results indicate that CCL299 might arrest cell-cycle progression at the G1/S transition.

Effects of CCL299 on the expression of cell-cycle regulators

Cyclin D–CDK4/6 and cyclin E–CDK2 complexes are active during the G1 phase and regulate the progression of the G1 phase (21). We examined the expression of regulatory proteins to confirm the impact of CCL299 on the progression of the G1 phase. CCL299 did not notably change the expression levels of G1 phase regulators, cyclin D1, CDK4, CDK6, cyclin E1, and CDK2 (Figure 5A). Moreover, p-CDK2 (Thr160), an activated form of CDK2 (22), was expressed markedly at a lower level in both HepG2 and HEp-2 cells (Figure 5A). These results were consistent with the speculation that CCL299 induces G1 phase arrest.

Cell stress frequently activates the p53–p21 pathway, which induces G1 phase arrest and apoptosis (23). We examined the expression levels of p21, p53, and p-p53 (Ser15), an activated form of p53 (31), to determine whether CCL299 affects these regulators. The expression levels of p21, p53, and p-p53 (Ser15) increased markedly (Figure 5B). CCL299 might cause G1 phase arrest followed by apoptosis due to the upregulation

of p21 and p-p53 (Ser15) and the downregulation of p-CDK2 (Thr160).

CCL299 did not inhibit the growth of A549 and TIG-1-20 cells; therefore, we examined the expression levels of p-CDK2 (Thr160), p21, p53, and p-p53 (Ser15) in these cells. CCL299 did not notably affect the expression levels of p-CDK2(Thr160), p21, p53, and p-p53 (Ser15) in A549 and TIG-1-20 cells (Figure 5C), indicating that CCL299 affects only specific cancer cell lines.

Effects of CCL299 on apoptosis

To further confirm that CCL299 induces apoptosis in HepG2 and HEp-2 cells, we determined caspase-3/7 activities using Caspase-Glo® 3/7 Assay kits. After 24-h treatment with 10 μM CCL299, the caspase-3/7 activities increased significantly (1.9-fold; $p<0.01$) only in HepG2 cells and increased 0.9-fold in HEp-2 cells. After 36-h CCL299 treatment, caspase-3/7 activities were elevated significantly in both cell lines (11- and 3.3-fold in HepG2 and HEp-2 cells, respectively; $p<0.01$). These results showed that CCL299-induced apoptosis in HepG2 and HEp-2 cells via modulation of caspase activities.

Discussion

We investigated CCL299 as a potential anticancer compound. In this study, CCL299

showed anticancer activity only for specific human cancer cell lines, without releasing cyanide anions. CCL299 induced cell-cycle arrest at the G1 phase, followed by apoptosis that was mediated through the p53-p21 pathway.

In this study, the IC_{50} values of CCL299 were 1.0 and 2.7 μmol/L for the human hepatoblastoma HepG2 and the human cervical cancer HEp-2 cells, respectively. In contrast, the IC_{50} values for human lung adenocarcinoma A549 and human fibroblast TIG-1-20 were both higher than 20 μmol/L. The results further indicated that CCL299 could mediate growth inhibition in cancer cells without releasing the cyano group because sodium thiosulfate treatment of CCL299-treated cancer cells did not restore cell viability. Inorganic cyanides exhibit rapid cytotoxicity by inactivating cytochrome oxidase (32); however, CCL299 showed time-dependent gradual cytotoxicity. Furthermore, this result supported the hypothesis that CCL299 did not release cyanide anions under the aforementioned experimental conditions. Therefore, CCL299 may be a safer anticancer compound despite containing a cyano group.

We further investigated the impact of CCL299 on cell-cycle progression and apoptosis. Unlike most benzimidazoles that are used as anticancer agents, CCL299 arrested cell-cycle progression at the G1 phase in HepG2 and HEp-2 cells. Studies of the mechanism of action of CCL299 demonstrated that CCL299 might activate the p53–p21 pathway in both HepG2 and HEp-2 cells. The cyclin E–CDK2 complex

regulates the G1-to-S-phase transition, and p21 suppresses this complex (23). In addition, an activated form of p53 (i.e., p-p53 (Ser15)), induces apoptosis (31). These facts suggest that the CCL299-induced strong induction of p21 and suppression of p-CDK2 (Thr160) might be sufficient to prevent cell-cycle progression from the G1 phase to the S phase, and that upregulation of p-p53 (Ser15) might suffice to induce apoptosis. In contrast, CCL299 had little effect on the expression levels of cell-cycle-related proteins in the human lung cancer cell line A549 and human TIG-1-20 fibroblasts. The precise mechanism of the specific cytotoxicity of CCL299 against HepG2 and HEp-2 remains unknown; however, cancer cells harbouring a subset of genetic alterations should be vulnerable to CCL299 (33, 34).

In conclusion, this study provides new and vital information that indicates that CCL299 has distinct mechanisms to suppress the proliferation of cancer cells. Therefore, CCL299 might be a worthy candidate that can be developed as a novel anticancer drug for the treatment of human hepatoblastoma and cervical cancer.

Acknowledgments

We are grateful to Dr. Takayoshi Arai (Department of Chemistry, Graduate School of Science, Chiba University) for the generous donation of reagents from Chiba Chemical Library (Chiba, Japan).

References

1 Bray F, Ferlay J, Soerjomataram I, Siegel RL, Torre LA and Jemal A. Global cancer statistics 2018: GLOBOCAN estimates of incidence and mortality worldwide for 36 cancers in 185 countries. CA Cancer J Clin 68*(6)*: 394–424, 2018. PMID: 30207593. DOI: 10.3322/caac.21492

2 Ferlay J, Colombet M, Soerjomataram I, Mathers C, Parkin DM, Piñeros M, Znaor A and Bray F. Estimating the global cancer incidence and mortality in 2018: GLOBOCAN sources and methods. Int J Cancer 144*(8)*: 1941–1953, 2019. PMID: 30350310. DOI: 10.1002/ijc.31937

3 Holohan C, Van Schaeybroeck S, Longley DB and Johnston PG. Cancer drug resistance: an evolving paradigm. Nat Rev Cancer 13*(10)*: 714–726, 2013. PMID: 24060863. DOI: 10.1038/nrc3599

4 Ramos P and Bentires-Alj M. Mechanism-based cancer therapy: resistance to therapy, therapy for resistance. Oncogene 34*(28)*: 3617–3626, 2015. PMID: 25263438. DOI: 10.1038/onc.2014.314

5 Vasan N, Baselga J and Hyman DM. A view on drug resistance in cancer. Nature 575*(7782)*: 299–309, 2019. PMID: 31723286. DOI: 10.1038/s41586-019-1730-

6 Akhtar W, Khan MF, Verma G, Shaquiquzzaman M, Rizvi MA, Mehdi SH, Akhter M

and Alam MM. Therapeutic evolution of benzimidazole derivatives in the last quinquennial period. Eur J Med Chem 126: 705–753, 2017. PMID: 27951484. DOI: 10.1016/j.ejmech.2016.12.010

7 Bansal Y and Silakari O. The therapeutic journey of benzimidazoles: a review. Bioorg Med Chem 20*(21)*: 6208–6236, 2012. PMID: 23031649. DOI: 10.1016/j.bmc.2012.09.013

8 Barot KP, Nikolova S, Ivanov I and Ghate MD. Novel research strategies of benzimidazole derivatives: a review. Mini Rev Med Chem 13*(10)*: 1421–1447, 2013. PMID: 23544603.

9 Keri RS, Hiremathad A, Budagumpi S and Nagaraja BM. Comprehensive review in current developments of benzimidazole-based medicinal chemistry. Chem Biol Drug Des 86*(1)*: 19–65, 2015. PMID: 25352112. DOI: 10.1111/cbdd.12462

10 Yadav G and Ganguly S. Structure activity relationship (SAR) study of benzimidazole scaffold for different biological activities: A mini-review. Eur J Med Chem 97: 419–443, 2015. PMID: 25479684. DOI: 10.1016/j.ejmech.2014.11.053

11 Schantz PM, Van den Bossche H and Eckert J. Chemotherapy for larval echinococcosis in animals and humans: report of a workshop. Z Parasitenkd 67*(1)*: 5–26, 1982. PMID: 7041454. DOI: 10.1007/BF00929509

12 Sadjjadi SM, Alborzi AW and Mostovfi H. Comparative clinical trial of mebendazole

and metronidazole in giardiasis of children. J Trop Pediatr 47*(3)*:176–178, 2001. PMID: 11419683. DOI: 10.1093/tropej/47.3.176

13 He L, Shi L, Du Z, Huang H, Gong R, Ma L, Chen L, Gao S, Lyu J and Gu H. Mebendazole exhibits potent anti-leukemia activity on acute myeloid leukemia. Exp Cell Res 369*(1)*: 61–68, 2018. PMID: 29750898. DOI: 10.1016/j.yexcr.2018.05.006

14 Sasaki J, Ramesh R, Chada S, Gomyo Y, Roth JA and Mukhopadhyay T. The anthelmintic drug mebendazole induces mitotic arrest and apoptosis by depolymerizing tubulin in non-small cell lung cancer cells. Mol Cancer Ther 1*(13)*:1201–1209, 2002. PMID: 12479701.

15 Doudican N, Rodriguez A, Osman I and Orlow SJ. Mebendazole induces apoptosis via Bcl-2 inactivation in chemoresistant melanoma cells. Mol Cancer Res 6*(8)*: 1308–1315, 2008. PMID: 18667591. DOI: 10.1158/1541-7786.MCR-07-2159

16 Stephenson LS, Latham MC, Adams EJ, Kinoti SN and Pertet A. Physical fitness, growth and appetite of Kenyan school boys with hookworm, Trichuris trichiura and Ascaris lumbricoides infections are improved four months after a single dose of albendazole. J Nutr 123*(6)*: 1036–1046, 1993. PMID: 8505663. DOI: 10.1093/jn/123.6.1036

17 Pourgholami MH, Woon L, Almajd R, Akhter J, Bowery P and Morris DL. In vitro and in vivo suppression of growth of hepatocellular carcinoma cells by albendazole.

Cancer Lett 165*(1)*:43–49, 2001. PMID: 11248417. DOI: 10.1016/s0304-3835(01)00382-2

18 Zhang X, Zhao J, Gao X, Pei D and Gao C. Anthelmintic drug albendazole arrests human gastric cancer cells at the mitotic phase and induces apoptosis. Exp Ther Med 13*(2)*: 595–603, 2017. PMID: 28352336. DOI: 10.3892/etm.2016.3992

19 Ghasemi F, Black M, Vizeacoumar F, Pinto N, Ruicci KM, Le CCSH, Lowerison MR, Leong HS, Yoo J, Fung K, MacNeil D, Palma DA, Winquist E, Mymryk JS, Boutros PC, Datti A, Barrett JW and Nichols AC. Repurposing albendazole: new potential as a chemotherapeutic agent with preferential activity against HPV-negative head and neck squamous cell cancer. Oncotarget 8*(42)*: 71512–71519, 2017. PMID: 29069723. DOI: 10.18632/oncotarget.17292

20 Wang LJ, Liou LR, Shi YJ, Chiou JT, Lee YC, Huang CH, Huang PW and Chang LS. Albendazole-induced SIRT3 upregulation protects human leukemia K562 cells from the cytotoxicity of MCL1 suppression. Int J Mol Sci 21*(11)*: 3907, 2020. PMID: 32486166. DOI: 10.3390/ijms21113907

21 Sherr CJ. G1 phase progression: cycling on cue. Cell 79*(4)*: 551–555, 1994. PMID: 7954821. DOI: 10.1016/0092-8674(94)90540-1

22 Fang F, Orend G, Watanabe N, Hunter T and Ruoslahti E. Dependence of cyclin E-CDK2 kinase activity on cell anchorage. Science 271*(5248)*: 499–502, 1996. PMID:

8560263. DOI: 10.1126/science.271.5248.499

23 Karimian A, Ahmadi Y and Yousefi B. Multiple functions of p21 in cell cycle, apoptosis and transcriptional regulation after DNA damage. DNA Repair (Amst) 42: 63–71, 2016. PMID: 27156098. DOI: 10.1016/j.dnarep.2016.04.008

24 Sánchez-Martínez C, Lallena MJ, Sanfeliciano SG and de Dios A. Cyclin dependent kinase (CDK) inhibitors as anticancer drugs: Recent advances (2015-2019). Bioorg Med Chem Lett 29*(20)*: 126637, 2019. PMID: 31477350. DOI: 10.1016/j.bmcl.2019.126637

25 Kasi PD, Tamilselvam R, Skalicka-Woźniak K, Nabavi SF, Daglia M, Bishayee A, Pazoki-Toroudi H and Nabavi SM. Molecular targets of curcumin for cancer therapy: an updated review. Tumour Biol 37*(10)*: 13017–13028, 2016. PMID: 27468716. DOI: 10.1007/s13277-016-5183-y

26 Poratti M and Marzaro G. Third-generation CDK inhibitors: A review on the synthesis and binding modes of Palbociclib, Ribociclib and Abemaciclib. Eur J Med Chem 172: 143–153, 2019. PMID: 30978559. DOI: 10.1016/j.ejmech.2019.03.064

27 Yi R, Ohno Y, Zheng T, Guo S, Chen W, Ma X, Win NN, Li Q, Vahed M, Saito K, Nakamoto S, Suganami A, Isegawa N, Yoshida K, Harada S, Tamura Y, Nishida A and Shirasawa H. CCL113, a novel sulfonamide, induces selective mitotic arrest and apoptosis in HeLa and HepG2 cells. Oncol Rep 44*(6)*: 2770–2782, 2020. PMID:

33125152. DOI: 10.3892/or.2020.7805

28 Guo S, Ohno Y, Tsubosaka A, Vahed M, Yi R, Ma X, Li Q, Saito K, Nakamoto S, Muroyama R, Suganami A, Tamura Y, Tsuchida A, Arai T and Shirasawa H. A novel chiral compound CCL441 induces mitotic arrest and apoptosis in hepatoblastoma HepG2 cells. Am J Res Med Sci 5*(1)*: 1–5, 2020.

29 Chen W, Yi R, Vahed M, Ohno Y, Tian Z, Guo S, Ma X, Win NN, Li Q, Tsubosaka A, Saito K, Nakamoto S, Suganami A, Tamura Y, Arai T and Shirasawa H. Novel chiral chalcone analogs that induce M phase arrest and apoptosis in HeLa cells. Med Chem (Los Angeles) 9*(6)*:74–82, 2019.

30 Sauer SW and Keim ME. Hydroxocobalamin: improved public health readiness for cyanide disasters. Ann Emerg Med 37*(6)*: 635–641, 2001. PMID: 11385334. DOI: 10.1067/mem.2001.114315

31 Yogosawa S and Yoshida K. Tumor suppressive role for kinases phosphorylating p53 in DNA damage-induced apoptosis. Cancer Sci 109*(11)*: 3376–3382, 2018. PMID: 30191640. DOI: 10.1111/cas.13792

32 Yonetani T. Studies on cytochrome oxidase. I. Absolute and difference absorption spectra. J Biol Chem 235: 845–852, 1960. PMID: 13846567.

33 MacConaill LE, Campbell CD, Kehoe SM, Bass AJ, Hatton C, Niu L, Davis M, Yao K, Hanna M, Mondal C, Luongo L, Emery CM, Baker AC, Philips J, Goff DJ, Fiorentino

M, Rubin MA, Polyak K, Chan J, Wang Y, Fletcher JA, Santagata S, Corso G, Roviello F, Shivdasani R, Kieran MW, Ligon KL, Stiles CD, Hahn WC, Meyerson ML and Garraway LA. Profiling critical cancer gene mutations in clinical tumor samples. PLoS One 4*(11)*: e7887, 2009. PMID: 19924296. DOI: 10.1371/journal.pone.0007887

34 Berger AH, Brooks AN, Wu X, Shrestha Y, Chouinard C, Piccioni F, Bagul M, Kamburov A, Imielinski M, Hogstrom L, Zhu C, Yang X, Pantel S, Sakai R, Watson J, Kaplan N, Campbell JD, Singh S, Root DE, Narayan R, Natoli T, Lahr DL, Tirosh I, Tamayo P, Getz G, Wong B, Doench J, Subramanian A, Golub TR, Meyerson M and Boehm JS. High-throughput phenotyping of lung cancer somatic mutations. Cancer Cell 30*(2)*: 214–228, 2016. PMID: 27478040. DOI: 10.1016/j.ccell.2016.06.022

Table

Table I. *Estimated IC_{50} values after 24-hour CCL299 treatment of HepG2, HEp-2, A549, and TIG-1-20 cells*

Species	Origin	Designation	IC_{50} (μmol/L)
Human	Hepatoblastoma cells	HepG2	1.0
	Cervical cancer cells; HeLa derivative	HEp-2	2.7
	Lung adenocarcinoma cells	A549	>20

Fibroblasts	TIG-1-20	>20

Figures

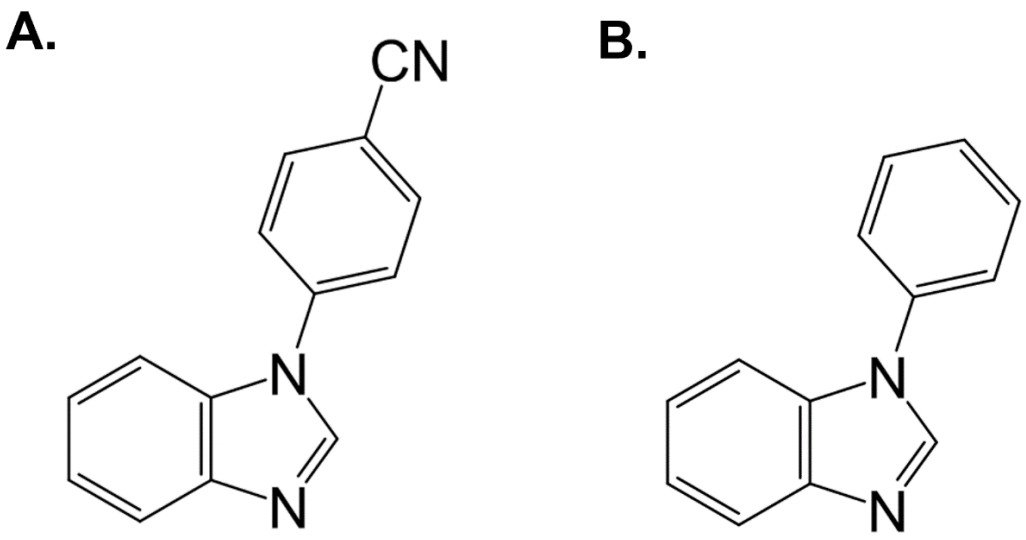

Figure 1. *The chemical structures of **(A)** CCL299, 4-(1H-1,3-benzodiazol-1-yl)benzonitrile, and **(B)** CCL937, 1-Phenyl-1H-benzoimidazole.*

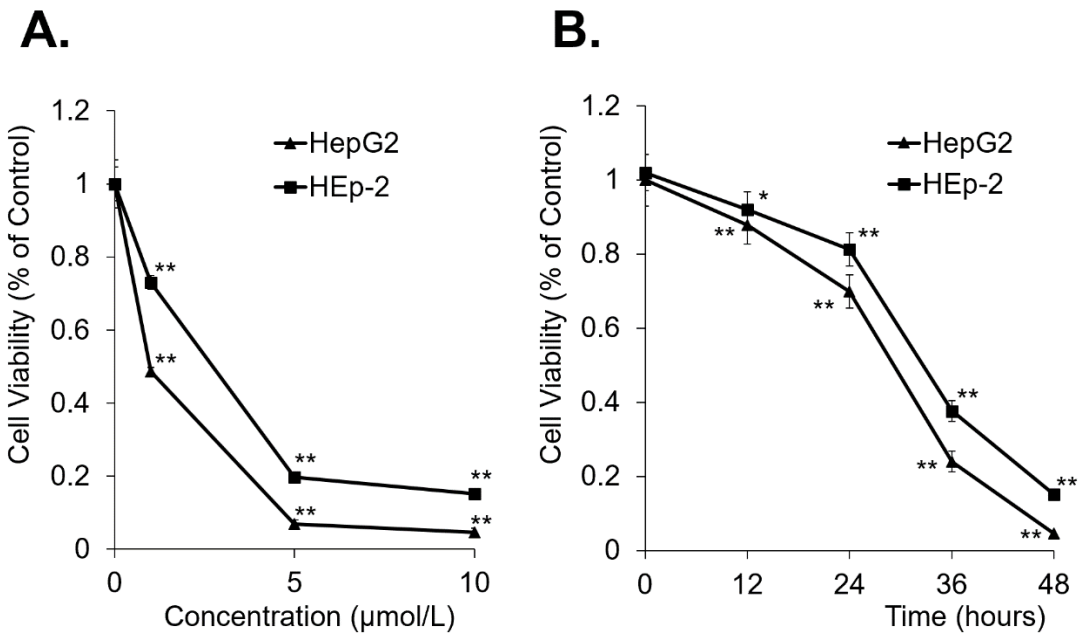

Figure 2. *Growth inhibition of CCL299 in HepG2 and HEp-2 cells. (**A**) The cell viabilities were determined by ATP assays. Human hepatoblastoma HepG2 cells and human cervical cancer HEp-2 cells were treated with 1, 5, and 10 μmol/L CCL299 or DMSO (vehicle control, 0 μmol/L) for 48 hours. (**B**) The cell viabilities were determined by ATP assays. HepG2 and HEp-2 cells were treated with 10 μmol/L CCL299 or DMSO as vehicle control (0 μmol/L) for different durations. *p<0.05, **p<0.01, compared with 0 μmol/L and 0 hour, respectively.*

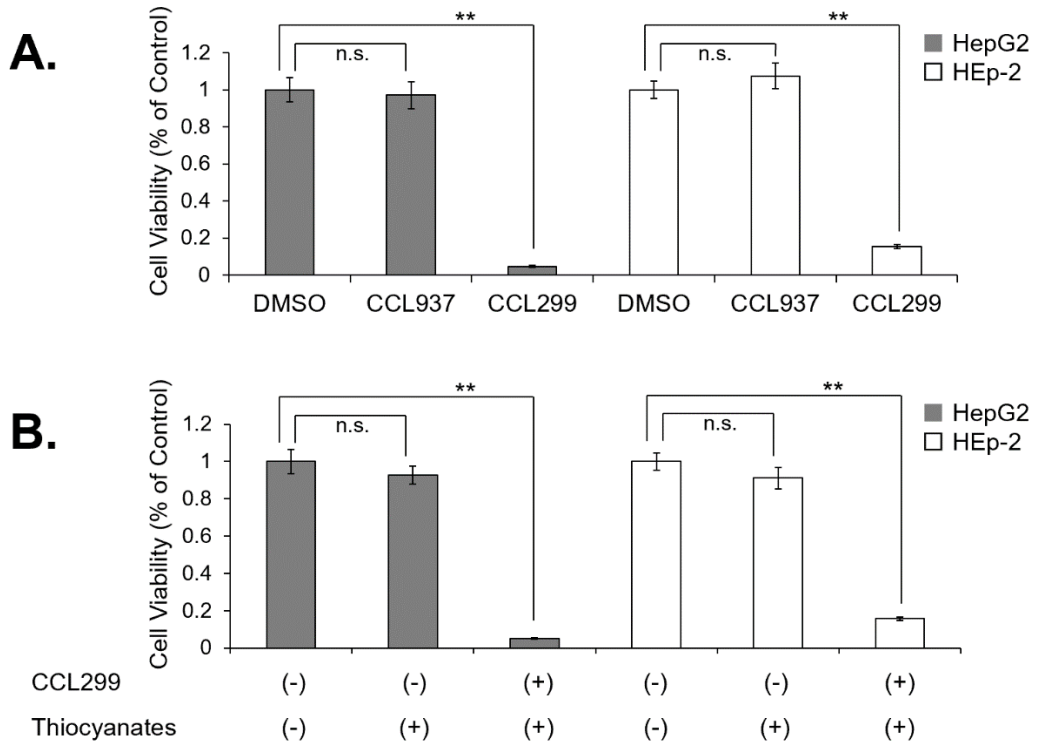

Figure 3. *Cytotoxicity of CCL299 in HepG2 and HEp-2 cells without the release of cyanide anions. (**A**) The cell viabilities were determined by ATP assays. HepG2 cells*

*and HEp-2 cells were treated with CCL299 (10 μmol/L), CCL937 (10 μmol/L), or DMSO (Control) for 48 hours. (**B)** The cell viabilities were determined by ATP assays. HepG2 cells and HEp-2 cells were treated with DMSO, CCL299 (10 μmol/L) and DMSO, or CCL299 (10 μmol/L) and sodium thiosulfate (1 mmol/L) for 48 hours. **p<0.01, compared with the DMSO-treated control.*

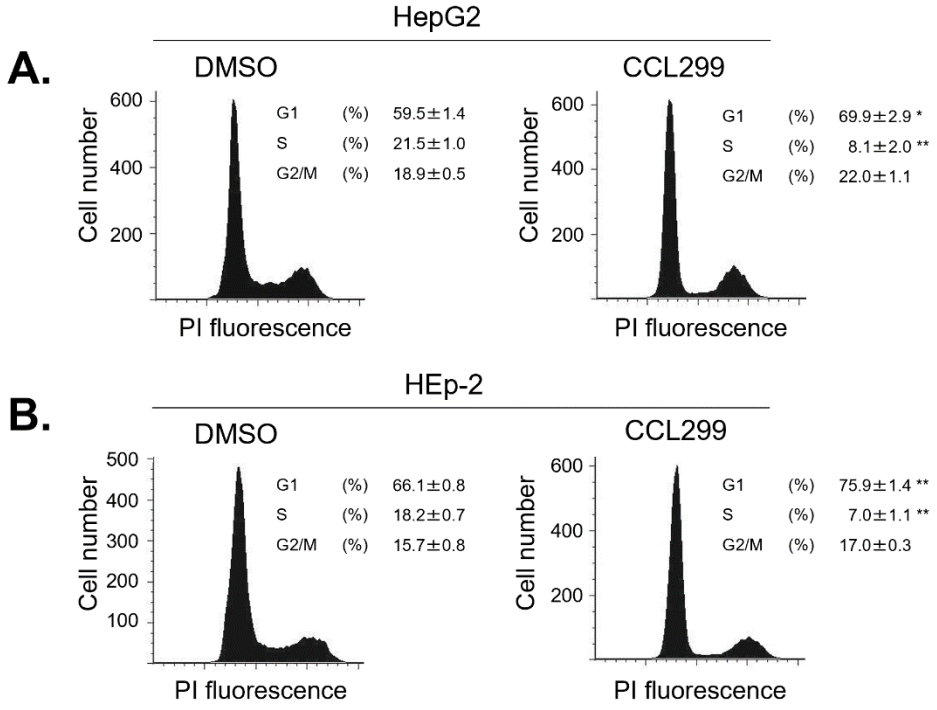

Figure 4. *Effects of CCL299 on cell-cycle arrest in HepG2 and HEp-2 cells. Cells from both cell lines were treated with 10 μmol/L CCL299 for 24 hours and subjected to flow cytometry. (**A)** Flow cytometry results of CCL299-treated and DMSO (control)-treated HepG2 cells. Percentages of cells in the G1, S, and G2/M phases are shown. (**B)** Flow cytometry results of CCL299-treated and DMSO (control)-treated HEp-2 cells. The*

*percentages of cells in the G1, S, and G2/M phases are shown. *p<0.05, **p<0.01, compared with the DMSO-treated control.*

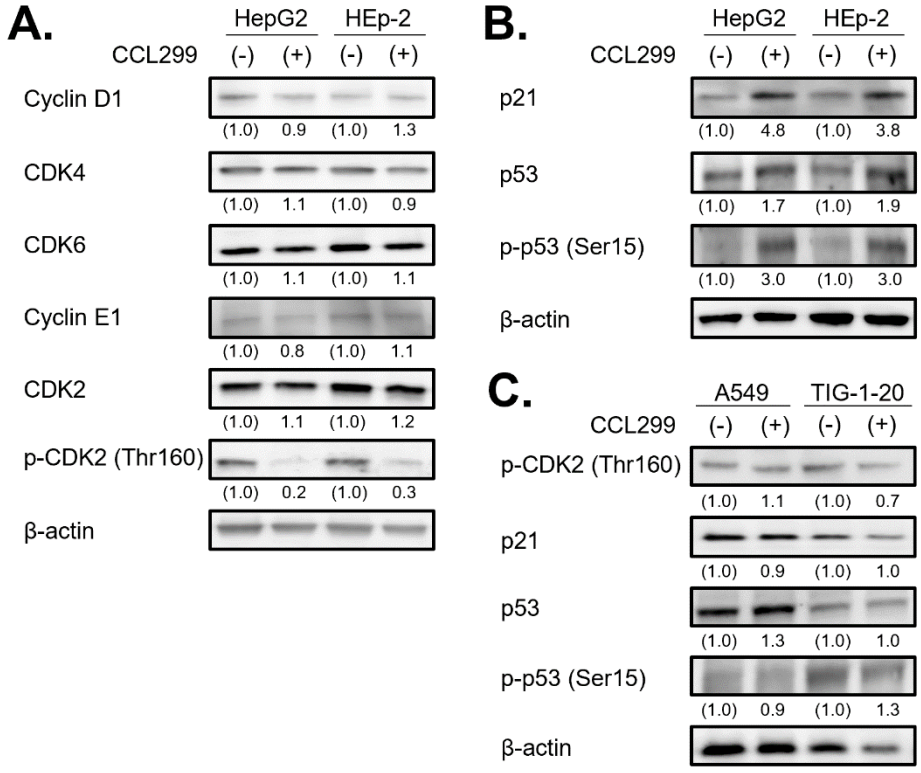

Figure 5. *Expression levels of the cell-cycle-related proteins in CCL299-treated cells. The expression levels of cell-cycle regulator proteins of CCL299-treated (10 μmol/L) or DMSO-treated HepG2 and HEp-2 cells were assessed by Western blot analysis. The total protein samples from CCL299-treated and DMSO-treated cells at 24 hours post-treatment were subjected to Western blotting. (**A)** Western blots of cyclin D1, CDK4, CDK6, cyclin E1, CDK2, and p-CDK2 (Thr160) in HepG2 and HEp-2 cells. (**B)** Western blots of p21, p53, and p-p53 (Ser15) in HepG2 and HEp-2 cells. (**C)** Western*

blots of p-CDK2 (Thr160), p21, p53, and p-p53 (Ser15) in A549 and TIG-1-20 cells. Fold-change values (CCL299-treated/DMSO-treated) normalized to β-actin (internal control) are shown below each band.

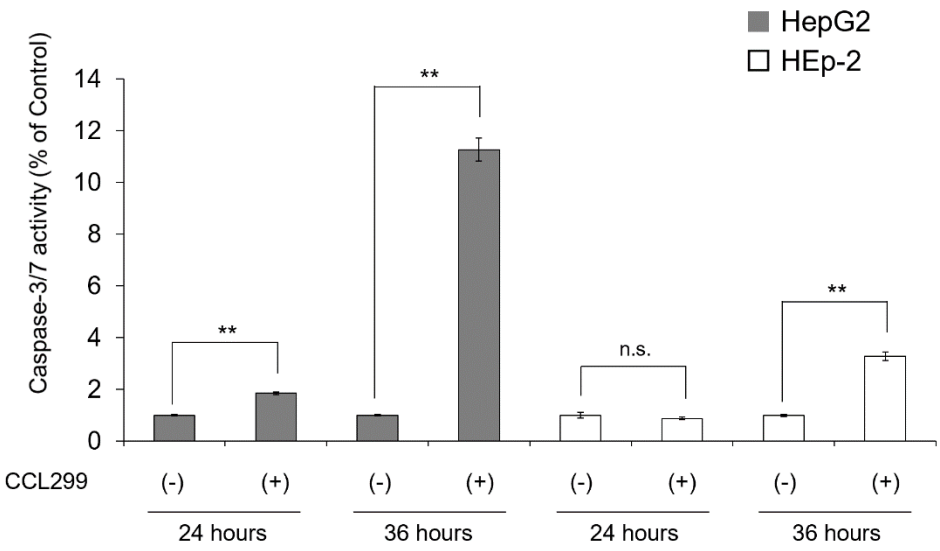

Figure 6. *Caspase-3/7 activities of CCL299-treated HepG2 and HEp-2 cells. Cells were treated with 10 μmol/L CCL299 for 24 or 36 hours. The ratios (CCL299-treated/DMSO-treated) are shown. **p<0.01, compared with the DMSO-treated control.*

Anticancer Research vol. 41 No. 2

2021 年 1 月 12 日　公表済

DOI: https://doi.org/10.21873/anticanres.14821